JOURNAL OF GEOPHYSICAL RESEARCH, VOL. 88, NO. C8, PAGES 4651–4662, MAY 30, 1983

Subsurface Energetics of the Gulf Stream Cyclonic Frontal Zone off Onslow Bay, North Carolina

CARROLL A. HOOD[1] AND JOHN M. BANE, JR.[2]

Marine Sciences Program, University of North Carolina, Chapel Hill, North Carolina 27514

It has been shown with the use of 4-month-long time series of velocity, temperature, and conductivity that fluctuating kinetic and potential energy was converted into kinetic and potential energy of the mean flow following a fluid particle in the subsurface Gulf Stream cyclonic frontal zone off Onslow Bay, North Carolina, during early 1979. This result agrees well with earlier measurements made in the surface layer off Onslow Bay. These flux calculations represent an important step in verifying the direction of the net cross-stream energy flux within the stream off Onslow Bay. According to an hypothesis presented for the growth and decay of Gulf Stream meanders along the continental margin of the southeastern United States, Onslow Bay is an area of decreasing meander amplitude. The direction of the energy conversion from meanders to the mean flow, determined from our calculations, is consistent with this hypothesis. Relatively low velocity covariances were found to be associated with relatively small transfers of kinetic energy during a period of low meander activity. This finding supports the notion that meanders play a significant role in the energy transformation processes. The presence of such 'quiet' periods may indicate a low-frequency modulation of Gulf Stream meander activity.

INTRODUCTION

The transfer of kinetic and potential energy between oceanic mean flows and fluctuations is an area of great interest in physical oceanography. A thorough investigation of energy transformation processes is essential to the understanding of ocean circulation in general. Theoretical studies of this phenomenon have identified processes capable of generating fluctuations [cf *Orlanski*, 1969; *Orlanski and Cox*, 1973; *Ikeda*, 1981] while observational studies have sought to delineate the energy pathways between these fluctuations and the mean flow in the real ocean [cf. *Webster*, 1961*b*, 1965; *Brooks and Niiler*, 1977; *Szabo and Weatherly*, 1979]. Analyses in the past, as well as in the present study, have centered around estimating terms in the fluctuation energy equation, which may be written

$$\frac{D}{Dt}\left[\frac{\langle u_i' u_i' \rangle}{2} + \frac{g/\rho(\langle \rho' \rho' \rangle/2)}{|\partial \rho/\partial z|}\right] = -\frac{\partial}{\partial x_i}\left(\frac{\langle u_i' p' \rangle}{\rho}\right) - \langle u_i' u_a' \rangle \left(\frac{\partial u_i}{\partial x_a}\right) - \frac{g/\rho \langle u_i' \rho' \rangle (\partial \rho/\partial x_i)}{|\partial \rho/\partial z|} \quad (1)$$

where $i, a = (1, 2, 3)$, 1, 2 being horizontal and 3 being vertical; $j = (1, 2)$, where 1, 2 are horizontal; $u_i = (u, v, w)$ the mean velocity component; $u_i' = (u', v', w')$, fluctuating velocity component; D/Dt is a substantial derivative; p' is fluctuating pressure; ρ is mean density; ρ' is fluctuating density; g is gravational acceleration; and angle brackets (e.g., $\langle\ \rangle$) denote time average. This equation states that a decrease (increase) in the fluctuation kinetic plus potential energy following the mean flow (first term) is due to loss (gain) by pressure work (second term) and conversion into (from) the kinetic (third term) and potential (last term) energy of the mean flow. Energetics investigations usually require a large amount of data for significant calculations, and many have been done in Western Boundary Currents (see *Niiler* [1975] for a recent review).

The earliest study addressing the question of the energy balance in the Gulf Stream was reported by *Webster* [1961*b*]. Using geomagnetic electrokinetograph (GEK) surface velocity data, he sought to calculate the kinetic energy flux across two Gulf Stream transects. The data for the study were from a transect across Onslow Bay and into the Gulf Stream (see Figure 1), and were compiled by *von Arx et al.* [1955]. During the 28-day investigation, 620 separate GEK surface velocity measurements were made. The data from a second transect across the Straits of Florida near Miami were gathered as part of a long-term project by the University of Miami. Between the years 1952 and 1958, 632 GEK surface velocity measurements were made. From these velocity measurements, *Webster* [1961*b*] calculated the transfer of kinetic energy between the fluctuations (meanders) and the mean flow due to the term $\langle u'v' \rangle (\partial v/\partial x)$. In each case he found the average cross-stream flux to be positive; that is, a flux of kinetic energy had occurred from the meanders to the mean flow, with maximum values measured in regions of high cyclonic shear. This result was somewhat surprising, as previous authors had suggested that the meanders derived their energy from the kinetic energy of the mean flow and represented a mechanism for 'frictional' dissipation of the current [*von Arx*, 1954; *Stommel*, 1965].

Webster [1965] followed up his previous study with data from two more transects, one across the Gulf Stream at 30°N off Jacksonville, Florida and a second consisting of a network of sections off Cape Hatteras, North Carolina. The first of these was surveyed by the R/V *Crawford* during a 1961 cruise. A total of 70 crossings were completed, during which continuous GEK measurements were taken. The data from

[1] Now at the Department of Oceanography, Florida State University, Tallahassee, Florida 32306.

[2] Also at the Department of Physics, University of North Carolina, Chapel Hill, North Carolina 27514.

Paper number 2C1844.
0148-0227/83/002C-1844$05.00

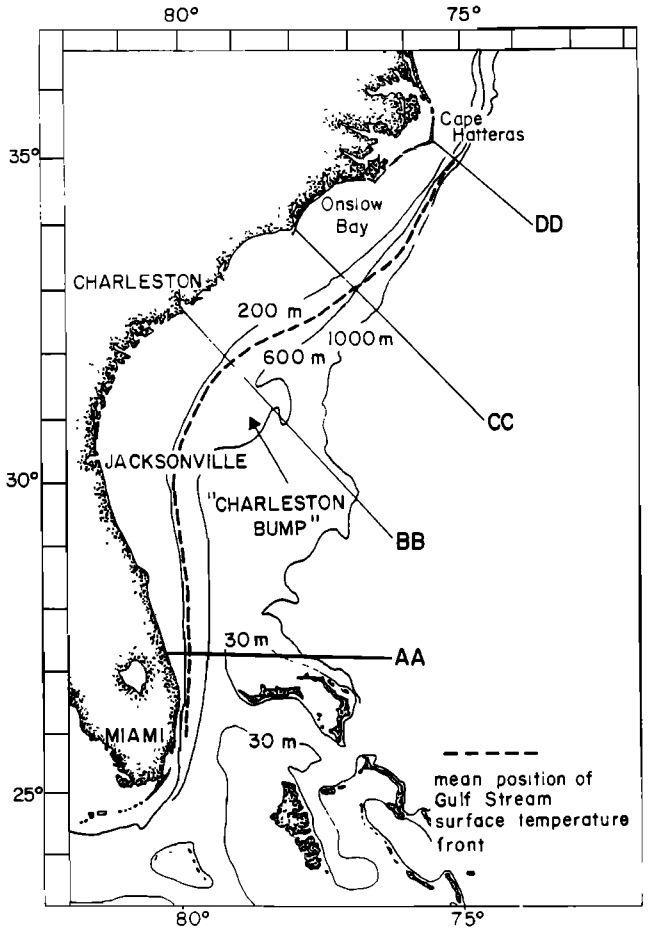

Fig. 1. The continental margin of the southeastern United States. The dotted line is the position of the mean shoreward Gulf Stream surface thermal front as calculated by *Bane and Brooks* [1979]. Double capital letters refer to sections along the thermal front as used in Figure 2. The 'Charleston bump' is the topographic feature between the 200-m and 600-m isobaths near 31°N.

the Hatteras transects were compiled by 20 crossings of an R/V *Crawford* cruise in 1962. Here, again, continuous GEK surface velocity measurements were made. The results were similar to the previous study. The largest contribution to the kinetic energy exchange due to the term $\langle u'v' \rangle (\partial v/\partial x)$ occurred in a 20-km-wide zone in the region of cyclonic shear. Outside this region there was little evidence of significant energy exchange in any direction. The cross-stream average remained positive for all transects, thereby indicating a transfer of energy from the fluctuations to the mean flow, although it is important to note that the Onslow Bay transect was the only one on which the magnitude of this exchange was significantly different from zero.

Using much of the same data as *Webster* [1965], *Oort* [1964] was able to calculate the conversion of available potential energy of the mean flow following the procedure described by *Lorenz* [1955]. In each case he found the direction of the flux to be from the fluctuations to the mean flow. He concluded that Gulf Stream meanders must have an outside energy source, since the meanders do not draw their energy from either the available potential energy or, according to *Webster*'s [1961*b*, 1965] results, the kinetic energy of the mean Gulf Stream.

The question of an external source of energy was addressed by *Schmitz and Niiler* [1969]. Using a free instrument technique [see *Schmitz and Richardson*, 1968], they collected velocity data along several crossings of a transect off Miami between 1964 and 1967 and along another transect near Jacksonville during 1967. Calculations of $\langle u'v' \rangle$ and $\langle u'v' \rangle (\partial v/\partial x)$ agreed well with the results obtained by *Webster* [1965]; however, cross-stream integration yielded a different result. Their results suggested a redistribution of kinetic energy between the fluctuations and the mean flow. That is, a substantial local exchange from the fluctuations to the mean flow occurred in regions of cyclonic shear with an equal amount transferred from the mean flow to the fluctuations in a wider zone spanning the rest of the current. This proposed internal adjustment requires no external energy source for the meanders to be present.

Brooks and Niiler [1977] supported *Schmitz and Niiler*'s [1969] results with their study of Florida Current energetics. Their data were collected from a combination of 53 free-drop transport profiles and numerous STD/XBT profiles taken in the Florida Current off Miami in 1974. They also used historical data from 12 cruises off Virginia Key made during 1965–1969. From these data they calculated and contoured several of the terms in the fluctuation energy equation (1). Typically, the flux terms showed large horizontal and vertical structure with positive and negative values occurring in all distributions. Additionally, as *Schmitz and Niiler* [1969] had earlier suggested, they found that area averages of the flux terms yielded little conversion of energy in either direction. Locally, energy conversion was found to be significant; however, no single term dominated the local balance. Rapid doubling times for the local fluctuation energy suggested that the pressure work terms must be included in the balance to accurately assess any local energy budget.

Brooks and Bane [1981, this issue] used current meter data to estimate the subsurface kinetic energy transfer at a fixed position over the continental slope off Onslow Bay. Energy flux calculations averaged over periods of about 110 days showed the direction of kinetic energy transfer to be from the fluctuations to the mean flow for both winter and summer, consistent with *Webster*'s [1961*b*] findings for the surface layer in that area. Another estimate of the energy flux was calculated for a 7-day portion of the 110-day winter record, characterized by intense meander activity. The conversion rate was significantly higher, implying that meanders play an important role in the conversion process.

The present paper describes results which extend those of *Brooks and Bane* [1981]. Both of these studies were part of the Gulf Stream Meanders Experiment (GSME), a theoretical and observational study designed to provide an understanding of the mesoscale meanders which propagate in the Gulf Stream as it flows along the continental margin of the southeastern United States. The GSME central objective was twofold: first, by using a combination of subsurface current meter time series, repeated airborne expendable bathythermograph (AXBT) and precision radiation thermometer (PRT) surveys, shipboard hydrographic surveys and satellite imagery, to determine the space-time characteristics of the subsurface temperature, salinity, and velocity fields in the stream as meanders propagate along the Carolina continental margin, and second, to assess the role of atmospherically or topographically induced long waves as the mechanism for producing the fluctuations (See *Bane et*

al. [1981] and *Brooks and Bane* [1981, this issue] for descriptions of GSME results and additional references.)

Gulf Stream meanders along the continental margin of the southeastern United States are vertically coherent, skewed wavelike motions that propagate northeastward (downstream) with phase speeds near 40 km d^{-1}. They typically have along-stream wavelengths of 90 to 260 km, peak to peak lateral amplitudes up to about 80 km, and dominant periods near 8 and 3 days [*Webster*, 1961*a*; *Vukovich and Crissman*, 1978; *Legeckis*, 1979; *Pietrafesa and Janowitz*, 1980; *Bane et al*, 1981; *Brooks and Bane*, 1981, this issue; *Lee et al.*, 1981]. A complete understanding of the processes by which meanders form is still unknown; however, several hypotheses describing meander growth have been proposed. One which we wish to consider in this paper is associated with a topographic irregularity in the continental slope between the 200 m and 600 m isobaths near 32°N, known as the 'Charleston bump' (see Figure 1). This feature is believed to be responsible for a seaward deflection of the Gulf Stream through a bottom steering effect [*Legeckis*, 1976, 1979; *Brooks and Bane*, 1978; *Pietrafesa et al.*, 1978; *Rooney et al.*, 1978; *Chao and Janowitz*, 1979; *Bane*, this issue]. Meanders present in the Stream upstream of the bump are apparently amplified as the Stream passes over the bump.

Bane and Brooks [1979] considered the amplification process by calculating the standard deviation of the position of the shoreward Gulf Stream surface thermal front from 64 weekly satellite composites [*NAVOCEANO*, 1976]. Figure 2 shows the standard deviation of the frontal position distribution as a function of distance along the mean frontal path. Note that the magnitude of the standard deviation rises slowly along the coast of Florida and Georgia (section AA to section BB), then increases sharply at approximately the latitude of the Charleston bump (section BB). Note also that the standard deviation curve reaches a maximum at the southern end of Onslow Bay (section CC), then begins to decrease toward Cape Hatteras (section DD).

This pattern suggests the following sequence for meander evolution along the southeastern United States. Small-amplitude meanders propagating northward from the Straits of Florida grow slowly as energy from the mean flow is converted to meander (fluctuation) energy through instability processes. Meander growth is restricted, however, due to the topographic constraint of the continental margin. According to the model studies of *Orlanski* [1969] and *Ikeda* [1981], the steep bottom slope will restrict the meander growth rate, which these studies indicate is due primarily to baroclinic instability. The topographic constraint is reduced downstream of Section BB as the stream is deflected seaward by the Charleston bump. In this region the increasing depth and decreasing bottom slope allow the stream to become more unstable, and there is the possibility of a relatively large conversion of mean energy to meander energy. As a result, the amplitudes of the meanders rapidly increase as they progress northeastward through the limited region between sections BB and CC in Figure 1. The continental slope steepens northward past Onslow Bay and, according to the mean surface front position in Figure 1, the stream flows closer to the outer edge of the shelf between sections CC and DD. This renewed topographic constraint restricts further meander growth, and requires that meander energy be converted back into mean energy, a process which results in decreasing meander amplitudes between Onslow Bay and Cape Hatteras. The bottom panel in Figure 2 depicts the direction of these implied energy fluxes.

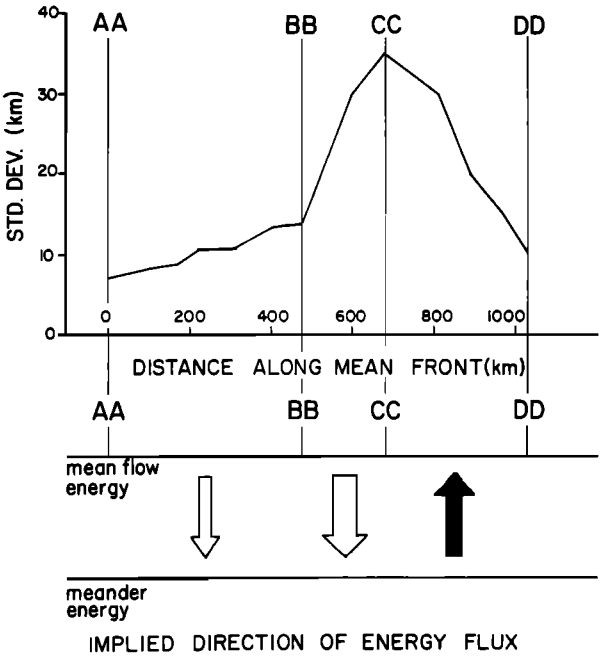

Fig. 2. The standard deviation of the position of the shoreward Gulf Stream surface thermal front as a function of distance along the mean front [after *Bane and Brooks*, 1979]. The locations of the section denoted by double capital letters are indicated on Figure 1. The bottom panel depicts the implied direction of energy transfer in the regions between these sections. The bold arrow is the one considered in this study.

The results of *Webster* [1961*b*, 1965] seem to contradict a portion of this hypothesis in that he found positive cross-stream kinetic energy exchange at all four of his Gulf Stream transects. Recall, however, that he calculated only one term in the fluctuation energy equation (1), and that the Onslow Bay transect was the only one where the flux due to this term was significantly different from zero. *Schmitz and Niiler*'s [1969] and *Brooks and Niller*'s [1977] results do not explicitly support this hypothesis, nor do they contradict it. The addition of other terms in their estimates (such as the pressure work terms) could easily shift the magnitude and sign of the cross-stream integrated flux. The study by *Hager* [1977] does lend support to the hypothesis. He calculated the kinetic energy of the mean flow and fluctuation energy in the surface layer of the Gulf Stream in 1° × 1° squares using historical ship drift data. Although his contours show considerable patchiness, meander energy reaches a maximum in the region south of Onslow Bay in the Stream's surface frontal zone.

In the present paper we present results which tend to support one portion of this hypothesis. Using subsurface velocity, temperature and conductivity data collected in the GSME, several of the terms in the fluctuation energy equation (1) were calculated. Our findings indicate that meander kinetic and potential energy was converted into mean flow energy in the subsurface cyclonic frontal zone of the Gulf Stream off Onslow Bay during early 1979. Coupled with similar findings by *Webster* [1961*b*, 1965] for the surface layer, these results suggest that the meanders which propagate northeastward past Onslow Bay must have been ener-

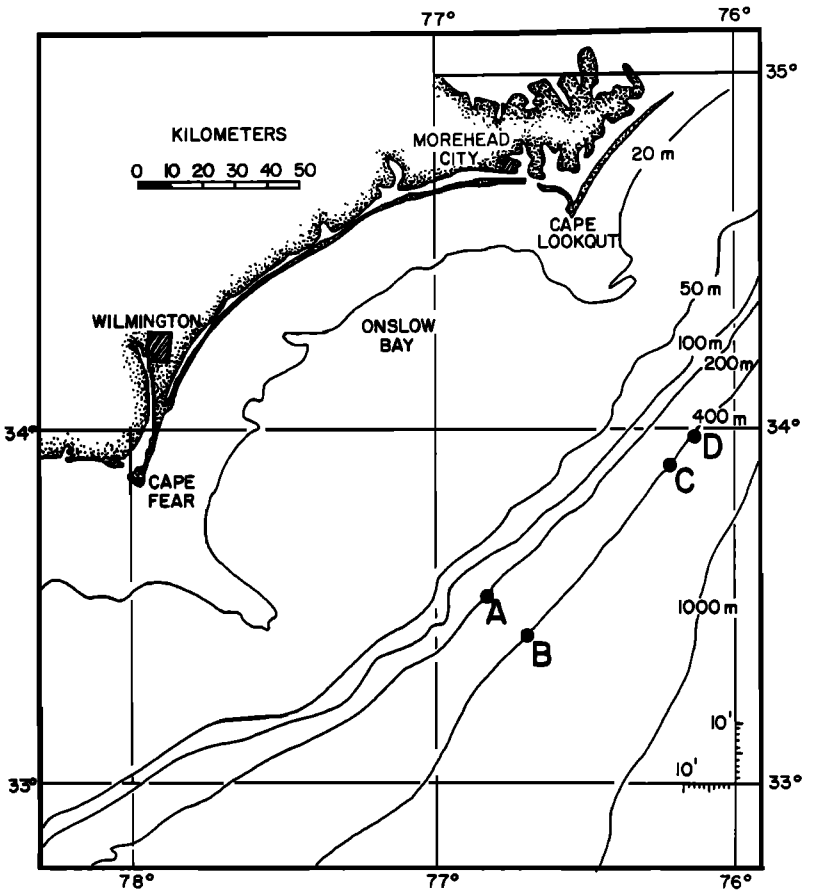

Fig. 3. The study area off Onslow Bay. The letters A, B, C, and D show the positions of the four current meter moorings.

gized upstream, only to lose their energy to the mean Stream as they progress towards Cape Hatteras.

METHODS

The data used to calculate the terms in the fluctuation energy equation (1) were collected with an array of ten Aanderaa RCM4 current meters moored over the upper continental slope off Onslow Bay. The array consisted of four taut wire moorings (A, B, C, D) placed in an *L*-shaped configuration oriented with the local topography (Figure 3). The moorings were similar in design to those described by *Lee and Shutts* [1977]. The short leg (A–B) was 18 km long and the long leg (B–C–D) was 75 km long. The positioning of the current meters within the array is shown schematically in Figure 4. The current meters were deployed January 16, 1979 and recovered May 15, 1979, providing a total possible recording time of 120 days. Complete data sets are documented by *Brooks et al.* [1980].

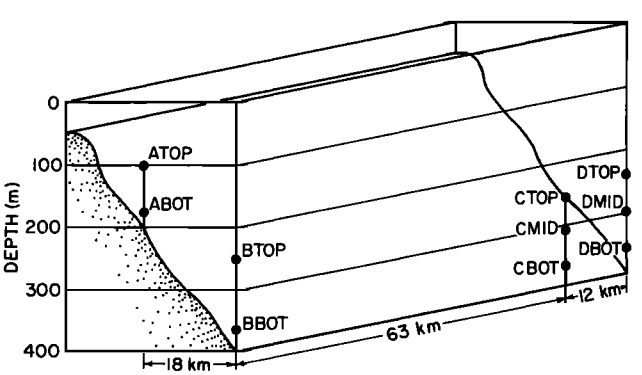

Fig. 4. The positioning of the current meters within the array.

Each current meter measured horizontal current speed and direction, temperature, and conductivity at 20-minute intervals. Additionally, the four 'top' current meters were each equipped with a pressure sensor. The resulting data sets consisted of time series of the four (five) parameters. Before deployment the current meters were calibrated with respect to temperature, direction, and pressure (where applicable). Best fit cubic polynomials derived from the calibration data were used to convert the original time series into those with scientific units. Calibration values supplied by the manufacturer were used in converting the recorded speed and conductivity series into scientific unit datasets. See *Brooks et al.* [1980] for tables of calibration coefficients and further details.

Salinity and density time series were generated for each meter using the temperature and conductivity time series [*Hood*, 1981]. The speed and direction time series were combined into offshore (u) and alongshore (v) velocity components aligned with the local 400-m isobath (034°T). Erroneous values in each time series were edited and replaced via linear interpolation. All time series were filtered using the FESTA time series analysis package [*Brooks*, 1976]. First, a 3-hour quarter-power-period Lanczos filter kernel was applied to reduce sampling noise and possible

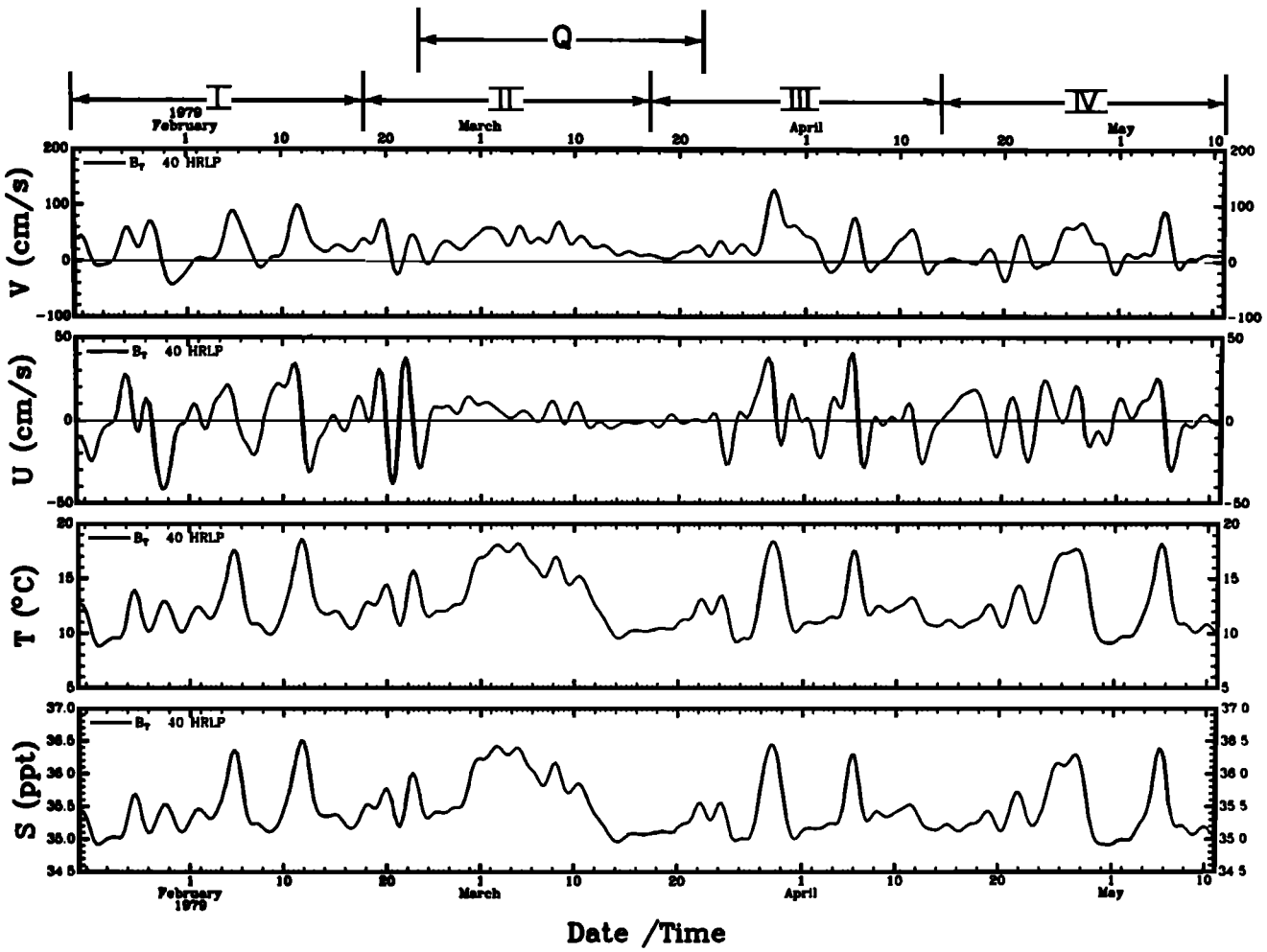

Fig. 5. Forty-hour low-pass time series for alongshore (v) and offshore (u) velocity components, temperature T and salinity S from the B_{TOP} current meter. The four averaging periods plus the quiet period are marked above the v record.

aliasing. Then a Lanczos 40-hour filter was applied to remove diurnal and semidiurnal tidal signatures, as well as those resulting from inertial motions. The resultant sample interval for the 40-hour low pass (40 HLP) data was 6 hours. Each of the 110-day-long 40-HLP series was divided into four periods (I through IV) of equal length in order to compare results from as many current meters as possible. Also, it appeared from the outset that there was a substantial length of time during which large-amplitude meander activity was at a minimum. Isolation of this 'quiet' period would permit comparison with a relatively 'active' period. Subsequently, a 27.5-day-long period was delineated as the quiet period Q (Figure 5).

The components of the pertinent six terms of the fluctuation energy equation (1) were calculated for periods I, II, III, and IV, plus cumulative periods I + II (E55), I + II + III (E83), I + II + III + IV (E110), and Q, the quiet period. All velocity and density values were decomposed into a mean component and a fluctuating component for each period. With this information, the appropriate covariances were calculated. The standard error (SE) of the mean for each time-averaged velocity, density, and covariance was calculated using the formula SE = (standard deviation)/$N^{1/2}$, where N is the number of values used in the calculation. Following the method of *Webster* [1961*b*, 1965] and *Brooks and Bane* [1981], only the standard error of a covariance was used to calculate the standard error of a energy flux term.

A finite difference technique was used to estimate most derivatives in the energy flux terms. Due to the array geometry, the x- and y-directed spatial derivatives were calculated at different points. There was but one choice for the x derivative, a combination of the A and B moorings, while several choices were available for the y derivatives. The B-C combination would have been spatially closet to the point where the x derivatives were calculated; however, due to the distances between moorings in the B-C and C-D mooring pairs, the C-D combination gave better estimations of y derivatives and was selected for the computations.

Although the selection of the C-D combination dictated that the x and y derivatives be calculated approximately 69 km apart, the positional differences can be rationalized in the following manner. Figure 6 gives a comparison of the velocity records of the top meters on the B and D moorings, B_{TOP} and D_{TOP}, for a portion of the January-February period. Given that the distance from B to D is 75 km and that the average propagation speed of meanders during this time was about 33.5 km $^{-1}$ [*Bane et al.*, 1981], a lead time of 54 hours has been applied to the D_{TOP} record. The signatures appear quite similar, suggesting that the fluctuations which occurred at mooring B also occurred at mooring D about 54

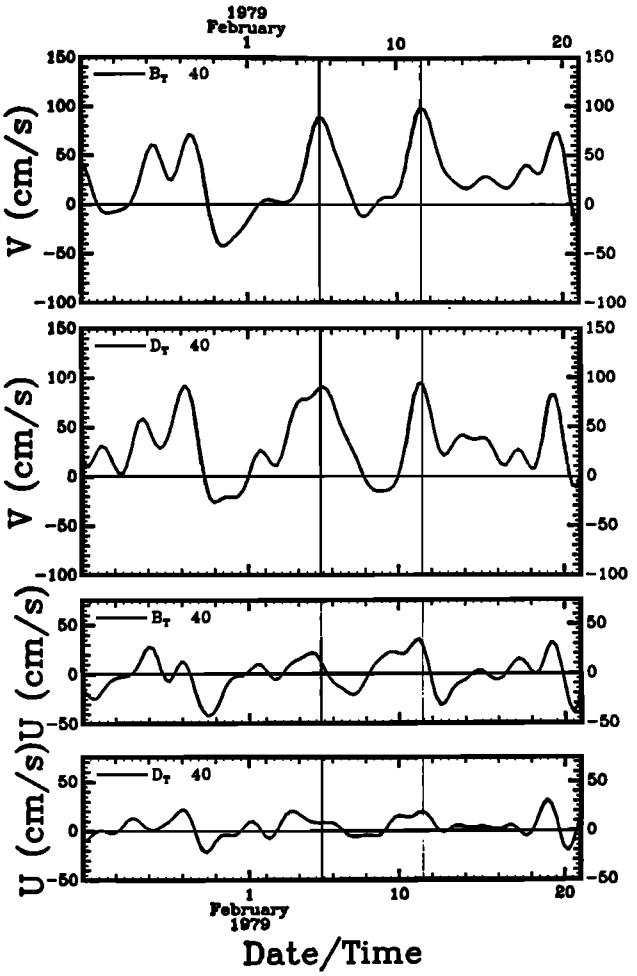

Fig. 6. Comparison of the u and v 40-HLP time series of B_{TOP} and D_{TOP} from January 22, to February 20, 1979. The D_{TOP} time series has a lead time of 54 hours applied. The vertical lines help illustrate the similarity between the two series during the passage of two meanders. Note the skewed velocity signatures shown in the records. They indicate a skewed wave motion, consistent with kinetic energy transfer from the fluctuations to the mean [after *Bane et al.*, 1981].

hours later. Compared with a record length of 27.5 days, 54 hours is relatively small; therefore the y derivatives calculated at the C-D mooring pair are believed to be representative of the same quantities which would have been calculated near the A-B mooring pair. Thus the use of the C-D combination for y derivatives and the A-B combination for x derivatives was chosen as the best approach for this particular array.

Initially, all logical combinations of A-B and C-D time series were to be used for finite difference calculations; i.e., C_{TOP}-D_{TOP}, C_{MID}-D_{MID}, C_{BOT}-D_{BOT} for y derivatives and A_{TOP}-B_{TOP}, A_{BOT}-B_{TOP}, A_{BOT}-B_{BOT} for x derivatives. However, currents measured with the bottom current meters usually had magnitudes much smaller than those measured with the other meters. Flux calculations made with these measurements were relatively small. *Brooks and Niiler* [1977] and *Brooks and Bane* [1981] encountered similar problems. Therefore the calculations using data from the bottom meters were discarded, with the exception of the A_{BOT}-B_{TOP} combination. Due to the array design, this combination contained the least amount of horizontal slope for the calculation of x derivatives (see Figure 4). The remaining combinations were C_{TOP}-D_{TOP}, C_{MID}-D_{MID} for y derivatives and A_{TOP}-B_{TOP}, A_{BOT}-B_{TOP} for x derivatives.

In calculating each energy flux term, the covariance was calculated at each of the meters used in the derivatives in the flux term. By then using each covariance, four calculations of each flux term were made. For example, the four combinations for the term $\langle u'u' \rangle$ $(\partial u/\partial x)$, are as follows:

Covariance	Derivative
B_{TOP}	B_{TOP}-A_{BOT}
A_{BOT}	B_{TOP}-A_{BOT}
B_{TOP}	B_{TOP}-A_{TOP}
A_{TOP}	B_{TOP}-A_{TOP}

This procedure was followed in calculating five of the six terms in the fluctuation energy equation (1). The exception was the term $(g/\rho)\langle u'\rho' \rangle$ $(\partial\rho/\partial x)/|\partial\rho/\partial z|$. Recall the differences in the depths of the current meters on the A and B moorings (Figure 4). This slope tends to underestimate the calculation of $\partial\rho/\partial x$, in some cases by almost an order of magnitude. Figure 7 shows a temperature cross section of the Gulf Stream contoured from AXBT data collected in the study area on February 14, 1979 [*Bane et al.*, 1980]. Line I parallels the line formed between moorings A and B and is the AXBT line closest to the actual position of the current meters. Note how the tilt of the isotherms is comparable to the tilt between the current meters. In order to circumvent the incorrect estimation of $\partial\rho/\partial x$ which would result from this current meter placement, the contoured data shown in Figure 7, along with similar sections constructed from flights on February 9, 11, 15, and 17, were used to determine the lateral and vertical temperature gradients at depths of 98 m

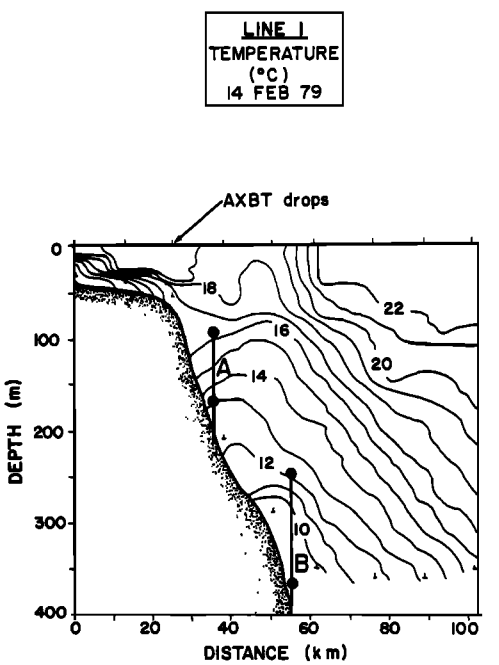

Fig. 7. Vertical temperature section through the Gulf Stream frontal zone constructed from AXBT data collected during a flight on February 14, 1979. The A and B moorings have been superimposed for reference. Note how the slope of the isotherms essentially follows the slope between the A and B current meters, thereby affecting the calculation of horizontal temperature gradients.

TABLE 1. Calculated Energy Fluxes (± One Standard Error) for the Term $\langle u'u' \rangle$ $(\partial u/\partial x)$

Period	α	β	γ	δ
I	−1.6 ± 0.2	−0.1 ± 0.0	−1.5 ± 0.2	−0.3 ± 0.1
II	3.1 ± 0.7	0.3 ± 0.0	2.8 ± 0.6	0.5 ± 0.1
III	6.2 ± 1.0	0.5 ± 0.1	1.1 ± 0.2	0.2 ± 0.0
IV	4.8 ± 0.6	0.9 ± 0.1	−0.8 ± 0.1	−0.2 ± 0.0
E110	4.3 ± 0.3	0.5 ± 0.0	1.3 ± 0.1	0.3 ± 0.0
E83	3.2 ± 0.3	0.3 ± 0.0	1.4 ± 0.1	0.3 ± 0.0
E55	1.7 ± 0.2	0.1 ± 0.0	1.6 ± 0.2	0.3 ± 0.0
Q	0.9 ± 0.3	0.2 ± 0.0	0.5 ± 0.1	0.3 ± 0.0

$\alpha = (B_{TOP})\ (B_{TOP}\text{-}A_{BOT})$; $\beta = (A_{BOT})\ (B_{TOP}\text{-}A_{BOT})$; $\gamma = (B_{TOP})\ (B_{TOP}\text{-}A_{TOP})$; $\delta = (A_{TOP})\ (B_{TOP}\text{-}A_{TOP})$. All flux values have been multiplied by 10^4; units are square centimeters per seconds squared. Data from various instrument combinations (α through δ) have been used for the calculations.

and 250 m, the depths of A_{TOP} and B_{TOP}, respectively. Using the T-S curve constructed from hydrographic data collected in the array area on the deployment cruise during January 1979 [*Brooks et al.*, 1980], salinity values were calculated, and these then used to calculate corresponding values of density. The derivatives $\partial\rho/\partial x$ and $\partial\rho/\partial z$ were averaged over all five flights. The averaged values were then used in the calculations of the term $(g/\rho)\ \langle u'\rho \rangle\ (\partial\rho/\partial x)/|\partial\rho/\partial z|$. The calculated value for $\partial\rho/\partial z$ was also used in the computation of $(g/\rho)\langle v'\rho' \rangle(\partial\rho/\partial y)/|\partial\rho/\partial z|$. Current meter data were used for $\langle u'\rho' \rangle$ and $\langle v'\rho' \rangle$ covariances (see Tables 5 and 6).

RESULTS

The estimates of the six calculable terms of the fluctuation energy equation (1) for all eight periods are given in Tables 1 through 6. The combinations of current meters used in each calculation are listed at the bottom of each table. The raw data used in the calculations are given in the appendix tables, A1 and A2.

The first four terms are the kinetic energy flux terms, the first of which is $\langle u'u' \rangle$ $(\partial u/\partial x)$(Table 1). All autocovariances are, of course, positive. Those of B_{TOP} are typically an order of magnitude greater than those of A_{BOT} and 3 to 5 times greater than those of A_{TOP}. The mean dilatation is positive in periods II, III, and Q, negative in period I, and changes sign in period IV. It is the same order of magnitude in all calculations (appendix). Consequently, the prevailing sense of this term is positive, indicating a transfer of energy from the meanders to the mean flow.

The next kinetic energy flux term is $\langle v'v' \rangle$ $(\partial v/\partial y)$, listed in Table 2. The autocovariances for all periods are positive and

TABLE 2. Calculated Energy Fluxes (± One Standard Error) for the Term $\langle v'v' \rangle$ $(\partial v/\partial y)$

Period	α	β	γ	δ
I	11.2 ± 1.1	11.9 ± 1.2	−17.4 ± 1.8	−16.2 ± 1.6
II	−0.9 ± 0.1	−1.1 ± 0.1	−11.0 ± 1.5	−13.6 ± 1.8
III	27.0 ± 4.6	32.2 ± 4.8		
IV				
E110				
E83	13.1 ± 0.9	15.1 ± 1.0		
E55	4.4 ± 0.3	4.9 ± 0.3	−15.8 ± 1.4	−16.2 ± 1.3
Q	−2.5 ± 0.3	−3.2 ± 0.4	−6.7 ± 1.0	−8.7 ± 1.3

$\alpha = (C_{MID})\ (D_{MID}\text{-}C_{MID})$; $\beta = (D_{MID})\ (D_{MID}\text{-}C_{MID})$; $\gamma = (C_{TOP})\ (D_{TOP}\text{-}C_{TOP})$; $\delta = (D_{TOP})\ (D_{TOP}\text{-}C_{TOP})$. See also footnote for Table 1.

TABLE 3. Calculated Energy Fluxes (± One Standard Error) for $\langle u'v' \rangle$ $(\partial u/\partial y)$

Period	α	β	γ	δ
I	0.0 ± 0.0	0.1 ± 0.0	−0.7 ± 0.1	−0.7 ± 0.1
II	−0.7 ± 0.2	−0.7 ± 0.1	−0.4 ± 0.1	−0.8 ± 0.2
III	−9.9 ± 2.5	−6.5 ± 2.5		
IV				
E110				
E83	−2.1 ± 0.4	−1.6 ± 0.4		
E55	−0.3 ± 0.1	−0.2 ± 0.1	−0.7 ± 0.1	−0.9 ± 0.1
Q	−0.4 ± 0.0	0.0 ± 0.1	−0.2 ± 0.1	−0.4 ± 0.1

$\alpha = (C_{MID})\ (D_{MID}\text{-}C_{MID})$; $\beta = (D_{MID})\ (D_{MID}\text{-}C_{MID})$; $\gamma = (C_{TOP})\ (D_{TOP}\text{-}C_{TOP})$; $\delta = (D_{TOP})\ (D_{TOP}\text{-}C_{TOP})$. See also Table 1 footnote.

have the same order of magnitude. They are generally one or two orders of magnitude greater than the covariances in the other kinetic energy flux terms. The sign of the mean dilatation shows great variability, probably because this particular derivative is calculated with velocity differences that are not much greater than the accuracy of the instruments. For this reason it is difficult to determine a prevailing sense for this term. *Szabo and Weatherly* [1979] suggested that this term has a sign opposite to that of $\langle u'v' \rangle$ $(\partial v/\partial x)$, which in our study would make it negative.

The third term examined is $\langle u'v' \rangle$ $(\partial u/\partial y)$, which is listed in Table 3. The crosscovariances are generally positive, consistent with the skewness and phase of the meander velocity signatures. The covariances at the top meters are nearly double those at the middle meters. The mean lateral shear is generally negative due to the curvature of the flow, thereby making the prevailing sense of this term negative. The contribution that this term makes to the overall energy transfer process is relatively small. *Brooks and Niiler* [1977] ignored this term altogether since $\partial v/\partial x$ is, in general, much greater than $\partial u/\partial y$.

The last kinetic energy flux term, $\langle u'v' \rangle$ $(\partial u/\partial y)$, generally dominates the kinetic energy exchange in the Gulf Stream [*Webster*, 1961*b*, 1965; *Schmitz and Niiler*, 1968; *Brooks and Niiler*, 1977]. It is listed in Table 4. The crosscovariances are positive for both A_{TOP} and B_{TOP} and mixed for A_{BOT}. The mean velocity shear is positive for all periods. As a result the prevailing sense of this term is positive.

The final two terms calculated are the potential energy flux terms. The first of these is $(g/\rho)\langle u'\rho' \rangle(\partial\rho/\partial x)/|\partial\rho/\partial z|$ and is listed in Table 5. The crosscovariances are nearly all negative and of the same order of magnitude. All of the calculations for this term used AXBT-derived values for each derivative, as noted in the section on methods. As in the

TABLE 4. Calculated Energy Fluxes (± One Standard Error) for $\langle u'v' \rangle$ $(\partial v/\partial x)$

Period	α	β	γ	δ
I	18.3 ± 7.5	6.7 ± 1.3	14.7 ± 6.0	13.2 ± 3.2
II	13.4 ± 4.9	2.3 ± 0.6	7.8 ± 2.8	1.7 ± 1.1
III	24.0 ± 6.5	−5.8 ± 0.9	20.4 ± 5.5	9.3 ± 2.5
IV	24.6 ± 2.0	−4.7 ± 0.7	48.4 ± 3.9	9.3 ± 3.1
E110	21.4 ± 2.8	−3.0 ± 0.7	18.8 ± 2.4	8.3 ± 0.1
E83	20.7 ± 3.9	−0.7 ± 0.9	15.1 ± 2.8	7.8 ± 1.4
E55	17.6 ± 4.6	4.6 ± 0.8	12.0 ± 3.1	7.0 ± 1.6
Q	8.4 ± 1.5	1.2 ± 0.5	3.7 ± 0.7	1.2 ± 0.7

$\alpha = (B_{TOP})\ (B_{TOP}\text{-}A_{BOT})$; $\beta = (A_{BOT})\ (B_{TOP}\text{-}A_{BOT})$; $\gamma = (B_{TOP})\ (B_{TOP}\text{-}A_{TOP})$; $\delta = (A_{TOP})\ (B_{TOP}\text{-}A_{TOP})$. See also Table 1 footnote.

TABLE 5. Calculated Energy Fluxes (± One Standard Error) for $(g/\rho)\langle u'\rho'\rangle(\partial\rho/\partial x)/|\partial\rho/\partial z|$

Period	α	β
I	4.5 ± 5.9	13.2 ± 9.6
II	−3.4 ± 2.0	12.6 ± 5.1
III	5.0 ± 3.6	24.3 ± 10.2
IV	14.6 ± 8.1	6.0 ± 8.1
E110	6.4 ± 3.1	16.5 ± 3.9
E83	1.4 ± 2.2	20.1 ± 4.5
E55	0.3 ± 3.1	19.8 ± 4.8
Q	4.8 ± 17.6	18.0 ± 3.0

$\alpha = (1/A_{TOP})(A_{TOP})$ (calculated)/(calculated); $\beta = (1/B_{TOP})(B_{TOP})$ (calculated)/(calculated). See also Table 1 footnote.

study by *Brooks and Niiler* [1977], we found the magnitude of this term to be about the same as that for $\langle u'v'\rangle(\partial v/\partial x)$. The prevailing sense of this term is positive, because the covariances and $\partial\rho/\partial x$ are both negative.

The last flux term considered is $(g/\rho)\langle v'\rho'\rangle(\partial\rho/\partial y)/|\partial\rho/\partial z|$ and is listed in Table 6. The crosscovariances are all negative and have the same order of magnitude. The great variability between the various combinations of the entire term comes from the calculation of $\partial\rho/\partial y$. The D_{TOP}-C_{TOP} combination gives a result at least one order of magnitude greater than the D_{MID}-C_{MID} combination. The larger values may not be unreasonable, as *Brooks and Niiler* [1977] stated that this term dominates the total conversion rate of potential energy. Therefore, despite some variability, most of the calculations suggest that the prevailing sense of this term is positive, indicating a transfer of potential energy from the fluctuations to the mean flow.

Although all of the terms showed some variability, the order of magnitude of the covariances were consistent with those found by *Brooks and Niiler* [1977] and *Webster* [1961*b*, 1965]. Four of the five significant terms tended to be positive, indicating an energy flux from the meanders to the mean flow. Due to nuances in finite differencing, estimates of the orders of magnitude may be tenuous. However, this most likely does not detract from the overall positive sense of the energy flux. Consider, for example, the term $\langle u'v'\rangle(\partial v/\partial x)$. It is clear that $\partial v/\partial x$ is positive in a region of cyclonic shear. From our measurements, cross-phase spectra show the weekly-period meanders to have velocity components which are about 60° out of phase, with v' lagging u', indicating that $\langle u'v'\rangle$ should be nonzero and positive [*Brooks et al.*, 1980]. Thus in the subsurface cyclonic frontal zone of the Gulf Stream off Onslow Bay, the direction of the energy transformation due to this term is found to be from the fluctuations to the mean flow.

This result agrees well with *Webster*'s [1961*b*] measurements in the surface frontal zone off Onslow Bay. This agreement is interesting in light of the results of *Bane et al.* [1981], which showed meander patterns in this region to be vertically coherent to depths of at least 400 m, thereby suggesting a subsurface meander energy flux similar to that in the surface layer. The spatial variability encountered in *Brooks and Niiler*'s [1977] Florida Straits profiles, however, prohibits one from speculating further on subsurface energetics from surface measurements. Additionally, more data are needed to accurately assess the subsurface cross-stream average energy fluxes off Onslow Bay. Until this is done, the direction of the bold arrow depicted in Figure 2 cannot be fully confirmed.

The quiet period is characterized by a noticable lack of large-amplitude meander signatures in the B_{TOP} time series (Figure 5). If, as *Webster* [1961*b*, 1965] and *Brooks and Bane* [1981] have suggested, the presence of meanders is central to fluctuation energy transformation, a comparison of this period with an active period should prove useful. Observing the term $\langle u'v'\rangle(\partial v/\partial x)$, it is found that period Q is characterized by typical v values but lower than normal $\langle u'v\rangle$ values (appendix). Two fairly active periods, I and IV (Figure 5), exhibit relatively high crosscovariances. The average cross-stream shear is about the same in both the quiet and active cases. This result suggests that the relatively small magnitude of kinetic energy transformation during the quiet period is due to small velocity crosscovariances, which is directly linked to the lack of meander activity.

This assertion raises an interesting question. Were meanders absent during the quiet period or did their signatures escape detection from the current meter array due to an offshore transgression of the Gulf Stream? Higher than average v measurements suggest an 'onshore' stream position and an apparent lack of meanders. However, an IR satellite image of the study area made March 18, 1979 during the late stages of the quiet period show the Gulf Stream to be well offshore of the array area, and to exhibit no meander patterns (Figure 8). Temperature and salinity measurements made at B_{TOP} (Figure 5) suggest that the stream was onshore near the beginning of the quiet period and slowly shifted offshore throughout the next few weeks. It appears likely, then, that the quiet period was indeed devoid of any large-amplitude meanders. Initial data from another 4-month-long mooring period (August to November 1979) off Onslow Bay show another slightly less active period in the velocity records [*Brooks and Bane*, this issue]. Whether or not this is a coincidence or supporting evidence of meander amplitude modulation by some low frequency oscillation remains to be determined.

A detailed comparison between the period I fluxes at the 250-m level and those of the quiet period may be made. Figure 9 shows the six calculable flux terms for each of these two periods in bar graph form. The standard errors of the terms are also displayed. It is immediately obvious that the period I fluxes total about three times the quiet period fluxes; 148.1 (± 39.2) × 10^{-4} cm^2 s^{-2} as compared to 52.2 (± 13.2) × 10^{-4} cm^2 s^{-2}. The largest energy flux during each period is the downstream conversion of potential energy (term 6). Due to the array design, this term, as well as other terms with y derivatives, is quite sensitive to slight changes

TABLE 6. Calculated Energy Fluxes (± One Standard Error) for $(g/\rho)\langle v'\rho'\rangle(\partial\rho/\partial y)/|\partial\rho/\partial z|$

Period	α	β	γ	δ
I	12.0 ± 1.5	12.3 ± 1.5	136.3 ± 20.0	109.8 ± 11.8
II	1.6 ± 0.8	1.3 ± 0.9	39.0 ± 14.2	28.5 ± 7.7
III	−12.2 ± 2.8	−13.2 ± 3.8		
IV				
E110				
E83	−2.3 ± 0.3	−2.3 ± 0.4		
E55	6.8 ± 1.1	7.0 ± 0.7	80.3 ± 8.4	62.8 ± 7.2
Q	0.1 ± 0.6	0.3 ± 0.6	31.8 ± 7.3	19.0 ± 6.0

$\alpha = (1/C_{MID})(C_{MID})(D_{MID}\text{-}C_{MID})$/(calculated); $\beta = (1/D_{MID})(D_{MID})(D_{MID}\text{-}C_{MID})$/(calculated); $\gamma = (1/C_{TOP})(C_{TOP})(D_{TOP}\text{-}C_{TOP})$/(calculated); $\delta = (1/D_{TOP})(D_{TOP})(D_{TOP}\text{-}C_{TOP})$/(calculated). See also Table 1 footnote.

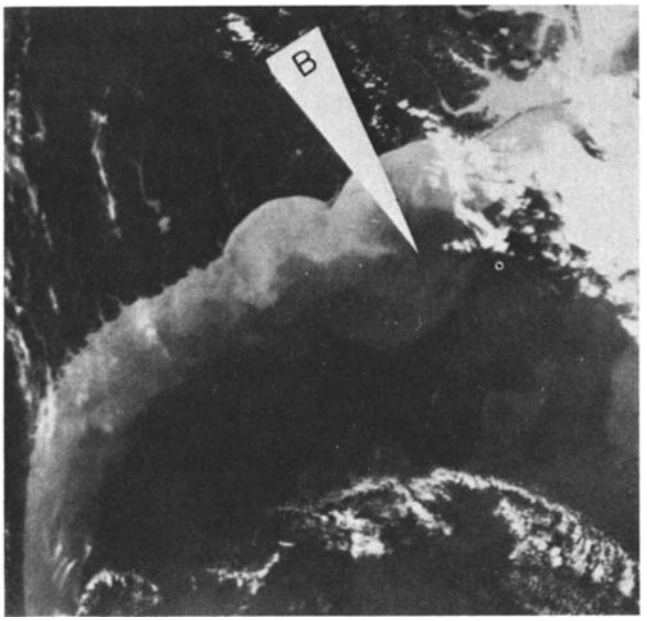

Fig. 8. Satellite composite of study area taken on March 18, 1979 near the end of the quiet period. The Gulf Stream surface thermal front is indicated by the black-grey interface. Note that the stream is well offshore of mooring B.

in the Gulf Stream's mean orientation. If only those terms containing x derivatives are used, the energy fluxes total 29.9 ($\pm$ 17.3) $\times$ 10^{-4} cm^2 s^{-2} for the period I and 27.3 ($\pm$ 4.8) $\times$ 10^{-4} cm^2 s^{-2} for the quiet period. These flux values indicate that energy was being converted from the fluctuations to the mean flow, with an insignificant reduction in the magnitude of the energy flux from period I to the quiet period. The fact that these flux calculations are similar in magnitude is due primarily to the fact that the cross-stream potential energy flux, term 5, was larger during the quiet period than during period I. This, in turn, is due to $\langle u'\rho' \rangle$ having a larger magnitude during the quiet period than in period I. We believe that this is associated with the apparent slow offshore shift of the stream during the quiet period.

SUMMARY AND DISCUSSION

It has been suggested with the use of 4-month-long time series of velocity, temperature, and conductivity that fluctuating kinetic and potential energy was converted into kinetic and potential energy of the mean flow, following a fluid particle, in the subsurface Gulf Stream cyclonic frontal zone off Onslow Bay, North Carolina, during early 1979. This result agrees well with similar measurements made at the surface off Onslow Bay by *Webster* [1961*b*, 1965]. These flux calculations represent an important step in verifying the direction of the net cross-stream energy flux within the stream off Onslow Bay. According to the hypothesis which we have presented for the growth and decay of Gulf Stream meanders along the continental margin of the southeastern United States, Onslow Bay is in the area of decreasing meander amplitude, as suggested by Figure 2. The direction of energy flux, from meanders to mean flow, determined from out calculations is consistent with this hypothesis. Additionally, relatively low velocity covariances (a remarkably consistent feature of the quiet period) were found to be associated with low meander activity and relatively small transfers of kinetic energy. This finding supports the notion that meanders play a significant role in the energy transformation processes. The presence of quiet periods within the velocity records may indicate a low frequency modulation of Gulf Stream meander activity.

Means, covariances, gradients, and flux terms were calculated for portions of the 110-day-long time series in order to assess the temporal variations in those quantities. Changes in a covariance term from one 27.5-day period (one quarter of the total record) to another was typically greater than the standard error of the covariance itself. Although this is due partially to our method of calculating the standard error, which assumes the measurements to be independent, it does reflect real changes in the fluctuation fields in the Gulf Stream. (Standard errors calculated with the assumption of dependence do not usually double the values.) The important result is that high velocity covariances are associated with large fluctuation velocities; that is, with high meander activity. The sign of the velocity covariances in most cases determines the direction of kinetic energy conversion, since the mean velocity gradients seldom change sign in this region. The velocity-density covariances show large changes from one 27.5-day period to another, as do the velocity

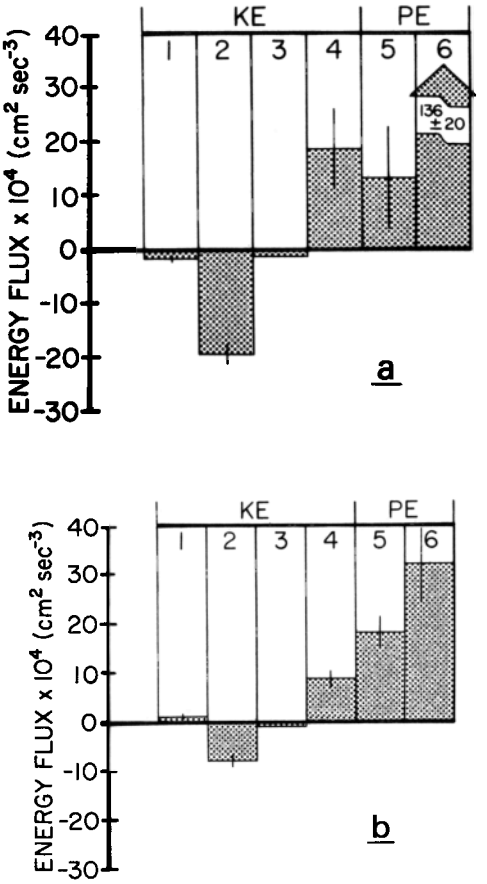

Fig. 9. The six calculable energy flux terms for (*a*) period I and (*b*) the quiet period displayed in bar graph form. The terms are numbered according to the fluxes listed in Tables 1–6. The x derivative term (terms 1, 4 and 5) are (B_{TOP}) (B_{TOP}-A_{BOT}) data, while the y derivative terms (term 2, 3, and 6) use (C_{TOP}) (D_{TOP}-C_{TOP}) data; thus these figures are indicative of the energy fluxes at about the 250-m level. The standard error of each flux term is shown by the vertical line at the top center of each bar.

covariances. In most cases relatively high velocity-density covariahces were found at times of high meander activity.

The meander amplification/decay hypothesis which we have considered here states that meanders progressing northward are amplified through instability processes which convert mean energy of the Gulf Stream into meander energy. The most rapid amplification occurs in the region just downstream of the Charleston bump. The energy flux then reverses direction between about the southern end of Onslow Bay and Cape Hatteras (sections CC and DD in Figure 1), and the meanders lose their energy as it is converted back to energy of the mean Gulf Stream. The flux terms which we have estimated from our Onslow Bay data indicate that this reconversion of energy occurs primarily through potential energy fluxes. Typical flux values may be seen in Figures 9*a* and 9*b*. These figures also show that nearly offsetting kinetic energy fluxes arise in terms 2 and 4 (see Tables 2 and 4, also).

As we have mentioned above, all y derivatives calculated here are to be viewed with caution, since the variable differences (e.g. Δv or $\Delta \rho$) are usually not much larger than the instrumental accuracy. An additional problem arises from the actual positioning of the instrument within the strongly baroclinic current. Velocity differences between two depths 10 m apart may be as great as those between two horizontal positions 10 km apart in the alongstream direction; thus small velocity differences become quite difficult to accurately determine with our field data.

If we do not consider the *y*-directed fluxes, then the direction of energy conversion remains the same, from fluctuations to mean flow. However, the energy conversion in this view is due to both potential and kinetic energy fluxes.

Due to the nature of our mooring array, which was not designed primarily to estimate energy fluxes, we cannot be more specific in stating the division between barotropic and baroclinic energy flux pathways in the reconversion processes off Onslow Bay. We do, however, feel confident in stating that our subsurface measurements clearly indicate an energy flux from meanders to mean flow, a result consistent with earlier measurements in the surface layer and with the spatial distribution of lateral meander amplitudes.

In light of the results summarized here, it is worthwhile to reiterate the major problems in this study so that they may be considered in future endeavors. They are as follows.

1. The positioning of the current meters within the array did not lend itself to accurate calculation of derivatives. The *x* derivatives contained some degree of tilt, and the *y* derivatives were calculated with differences in variables which were not much greater than the instrumental accuracies. The GSME was not designed with rigorous energetics calculations in mind, and future studies may wish to consider other array designs.

2. Current meter coverage permitted the estimation of a local energy flux budget only, while accurately assessing the direction of total energy transfer may require greater cross-stream coverage and several cross-stream transects.

3. Pressure work and vertical energy transfer terms could not be estimated with the present data set. As has been suggested in previous studies, these terms may be significant in a local energy budget, and methods to estimate these flux terms should be devised.

TABLE A1. Velocity, Density, and Covariance Values From the 40-Hour Low-Passed Time Series Used in the Energy Flux Calculations

Period	$\langle u'u' \rangle$, cm^2 s^{-2}	u, cm s^{-1}	$\langle u'v' \rangle$, cm^2 s^{-2}	v, cm s^{-1}	$\langle u'\rho' \rangle$, g cm^{-2} s^{-1} × 10^3
			A_{TOP}		
I	61.6 ± 10.1	0.14	119.0 ± 29.2	3.39	−0.17 ± 0.21
II	24.2 ± 3.1	−0.54	16.7 ± 11.1	13.8	0.12 ± 0.07
III	34.9 ± 5.7	−0.24	99.8 ± 26.9	9.94	−0.18 ± 0.13
IV	45.3 ± 5.4	1.09	81.3 ± 26.9	−4.80	−0.52 ± 0.29
E110	41.9 ± 3.4	0.11	79.4 ± 1.4	5.58	−0.23 ± 0.11
E83	40.3 ± 4.1	−0.21	77.3 ± 13.7	9.04	−0.05 ± 0.08
E55	43.0 ± 5.4	−0.20	66.1 ± 15.5	8.59	−0.01 ± 0.11
Q	24.5 ± 3.4	0.22	17.1 ± 10.7	16.0	−0.17 ± 0.63
			A_{BOT}		
I	18.2 ± 2.5	0.23	48.3 ± 9.4	−1.59	
II	12.8 ± 1.7	−0.85	13.2 ± 3.8	1.06	
III	17.1 ± 1.8	−4.80	−53.1 ± 7.8	7.01	
IV	31.3 ± 4.0	−4.85	−80.2 ± 11.7	5.27	
E110	25.1 ± 1.9	−2.57	−25.5 ± 6.1	2.94	
E83	20.7 ± 1.6	−1.81	−5.0 ± 6.2	2.16	
E55	15.8 ± 1.5	−0.31	30.0 ± 5.3	−0.27	
Q	11.6 ± 1.6	−1.38	7.7 ± 3.2	0.36	
			B_{TOP}		
I	275.2 ± 33.9	−0.84	132.1 ± 54.2	23.4	−0.44 ± 0.32
II	140.1 ± 29.9	3.08	78.2 ± 28.5	31.8	−0.42 ± 0.17
III	199.2 ± 32.2	0.77	218.3 ± 58.9	26.8	−0.81 ± 0.34
IV	170.1 ± 20.3	0.22	424.7 ± 33.9	15.7	−0.20 ± 0.27
E110	198.3 ± 15.0	1.29	179.4 ± 23.1	24.4	−0.55 ± 0.13
E83	207.4 ± 18.8	1.00	148.4 ± 27.8	27.3	−0.67 ± 0.15
E55	211.5 ± 23.2	1.12	113.4 ± 29.7	27.6	−0.66 ± 0.16
Q	48.4 ± 13.0	2.10	53.8 ± 9.8	28.5	−0.60 ± 0.10

TABLE A2. Velocity, Density, and Covariance Values From the 40-Hour Low-Passed Time Series Used in the Energy Flux Calculations

Period	$\langle v'v' \rangle$ cm^2 s^{-2}	v, cm s^{-1}	$\langle u'v' \rangle$, cm^2 s^{-2}	u, cm s^{-1}	$\langle v'\rho' \rangle$, g cm^{-2} s^{-1} × 10^3	σ_t
			C_{TOP}			
I	1239.4 ± 125.1	37.61	184.3 ± 29.2	4.71	−5.45 ± 0.80	27.03
II	511.6 ± 68.3	31.03	51.1 ± 17.4	4.81	−1.67 ± 0.61	26.96
III	893.3 ± 106.0	36.77	186.4 ± 32.5	5.29	−3.70 ± 0.36	27.05
IV	1548.3 ± 180.0	22.54	240.3 ± 41.7	1.29	−7.76 ± 0.56	26.99
E110	1084.3 ± 65.8	31.99	174.3 ± 16.6	4.03	−4.51 ± 0.30	26.96
E83	890.0 ± 62.7	35.14	140.8 ± 16.2	4.94	−3.50 ± 0.30	26.99
E55	886.3 ± 76.6	34.32	117.5 ± 17.6	4.76	−3.44 ± 0.36	26.99
Q	401.8 ± 61.6	29.10	28.6 ± 10.5	4.80	−1.27 ± 0.29	26.99
			C_{MID}			
I	780.2 ± 79.6	30.27	38.7 ± 18.6	−0.24	−2.39 ± 0.29	26.93
II	517.0 ± 63.6	17.74	55.7 ± 14.8	0.06	−0.47 ± 0.24	26.91
III	557.7 ± 95.5	22.57	121.8 ± 30.3	8.56	−1.46 ± 0.34	26.97
IV						
E110						
E83	645.6 ± 46.1	23.53	68.7 ± 13.5	2.80	−1.40 ± 0.17	26.90
E55	688.9 ± 50.1	24.00	46.3 ± 11.9	−0.09	−1.35 ± 0.21	26.92
Q	426.4 ± 59.1	17.90	35.6 ± 2.0	0.10	−0.03 ± 0.19	26.93
			D_{TOP}			
I	1160.7 ± 111.9	35.93	185.3 ± 29.0	4.26	−4.39 ± 0.47	26.88
II	631.3 ± 83.3	28.44	89.4 ± 21.9	3.78	−1.22 ± 0.33	26.82
III						
IV						
E110						
E83						
E55	910.0 ± 71.8	32.18	138.2 ± 18.4	4.02	−2.69 ± 0.31	26.85
Q	523.4 ± 79.3	27.10	51.2 ± 14.5	3.80	−0.76 ± 0.24	26.84
			D_{MID}			
I	826.7 ± 83.2	32.00	62.9 ± 17.4	−0.13	−2.46 ± 0.31	26.90
II	629.3 ± 75.9	17.53	55.8 ± 10.5	−1.42	−0.39 ± 0.26	26.89
III	665.3 ± 98.9	28.37	80.1 ± 30.9	−1.21	−1.58 ± 0.46	27.02
IV	975.9 ± 100.2	19.29	48.9 ± 27.6	−3.08	−2.53 ± 0.32	26.91
E110	811.0 ± 46.5	24.29	54.1 ± 11.9	−1.46	−1.62 ± 0.18	26.88
E83	744.9 ± 49.9	25.96	52.3 ± 12.6	−0.92	−1.35 ± 0.21	26.91
E55	780.4 ± 54.9	24.76	38.9 ± 10.9	−0.77	−1.39 ± 0.14	26.89
Q	542.3 ± 73.5	17.20	−1.2 ± 7.3	−1.20	−0.10 ± 0.19	26.91

Acknowledgments. The Gulf Stream Meanders Experiment was supported by the Office of Naval Research under contract N00014-77-C-0354, and by the National Science Foundation under grants OCE77-25682 and OCE 79-06710. Assistance during the field phases of the experiment was provided by several graduate students at the University of North Carolina, Texas A & M University and North Carolina State University. Paul Blankinship receives special thanks for his expert work with mooring preparation, deployment and recovery. We thank Thomas Reid for assistance with processing and plotting the time series data, Kimberly Clark for drafting, and Schatzie Fisher and Dianne Hamm for typing numerous drafts of the manuscript. We also extend our appreciation to the crew of the R/V *Endeavor* for their effective services at sea.

REFERENCES

Bane, J. M., Jr., Initial observations of the subsurface structure and short-term variability of the seaward deflection of the Gulf Stream off Charleston, South Carolina, *J. Geophys. Res.*, this issue.

Bane, J. M., Jr., and D. A. Brooks, Gulf Stream meanders along the continental margin from the Florida Straits to Cape Hatteras, *Geophys. Res. Lett.*, *6*, 280–282, 1979.

Bane, J. M., Jr., D. A. Brooks, K. R. Lorenson, and C. M. Seay, The Gulf Stream Meanders Experiment: AXBT/PRT data report, R/A Project Birdseye flights 9–18 February, 1979, *Rep. CMS-80-2*, Univ. of N. C., Chapel Hill, 1980.

Bane, J. M., Jr., D. A. Brooks, and K. R. Lorenson, Synoptic observations of the three dimensional structure and propagation of Gulf Stream meanders along the Carolina continental margin, *J. Geophys. Res.*, *86*, 6411–6425, 1981.

Brooks, D. A. (editor), *Festa at NCSU*, Center for Marine and Coastal Studies, North Carolina State University, Raleigh, North Carolina, 1976.

Brooks, D. A., and J. M. Bane, Jr., Gulf Stream deflection by a bottom feature off Charleston, South Carolina, *Science*, *201*, 1225–1226, 1978.

Brooks, D. A., and J. M. Bane, Jr., Gulf Stream fluctuations and meanders over the Onslow Bay upper continental slope, *J. Phys. Oceanogr.*, *11*, 247–256, 1981.

Brooks, D. A., and J. M. Bane, Jr., Gulf Stream meanders off North Carolina during winter and summer, 1979, *J. Geophys. Res.*, this issue.

Brooks, D. A., J. M. Bane, R. L. Cohen, and P. Blankinship, The Gulf Stream Meanders Experiment: Current meter, atmospheric, and sea level data report for the January to May, 1979 mooring period, *Rep. 80-7-T*, Texas A & M Univ., College Station, Tex., 1980.

Brooks, I. H., and P. P. Niiler, Energetics of the Florida Current, *J. Mar. Res.*, *35*, 163–191, 1977.

Chao, S. Y., and G. S. Janowitz, The effect of a localized topographic irregularity on the flow of a boundary current along the continental margin, *J. Phys. Oceanogr.*, *9*, 900–910, 1979.

Hager, J. G., Kinetic energy exchange in the Gulf Stream, *J. Geophys. Res.*, *82*, 1710–1724, 1977.

Hood, C. A., Subsurface energetics of the cyclonic Gulf Stream

frontal zone off Onslow Bay, North Carolina, M. S. thesis, Univ. of N. C., Chapel Hill, 1981.
Ikeda, M., Meanders and detached eddies of a strong eastward-flowing jet using a two-layer quasi-geostrophic model, *J. Phys. Oceanogr., 11*, 526–540, 1981.
Legeckis, R. V., The influence of bottom topography on the path of the Gulf Stream at latitude 31 N from NOAA's satellite imagery, *Eos Trans. AGU, 57*, 260, 1976.
Legeckis, R. V., Satellite observations of the influence of bottom topography on the seaward deflection of the Gulf Stream off Charleston, South Carolina, *J. Phys. Oceanogr., 9*, 483–497, 1979.
Lee, T. N., and R. L. Shutts, Technical program for Aanderaa current meter moorings on continental shelves, *Tech. Rep. No. TR-77-5*, Univ. of Miami, Miami, Fla., 1977.
Lee, T. N., L. P. Atkinson, and R. V. Legeckis, Observations of a Gulf Stream frontal eddy on the Georgia continental shelf, April 1977, *Deep Sea Res., 28A*, 347–378, 1981.
Lorenz, E. N., Available potential energy and the maintenance of the general circulation, *Tellus, 7*, 157–167, 1955.
NAVOCEANO, Experimental Ocean Frontal Analysis charts, U. S. Naval Oceanogr. Off., Washington, D. C., 1976.
Niiler, P. P., Variability in western boundary currents, in *Numerical Models of Ocean Circulation*, National Academy of Sciences, Washington, 1975.
Oort, A. H., Computations of the eddy heat and density transports across the Gulf Stream, *Tellus, 16*, 55–63, 1964.
Orlanski, I., The influence of bottom topography on the stability of jets in a baroclinic fluid, *J. Atmos. Sci., 26*, 1216–1232, 1969.
Orlanski, I., and M. D. Cox, Baroclinic instability in ocean currents, *Geophys. Fluid Dyn., 4*, 297–332, 1973.
Pietrafesa, L. J. and G. S. Janowitz, On the dynamics of the Gulf Stream front in the Carolina Capes, in *Stratified Flows: The Second International Symposium on Stratified Flows*, Tapen, New York, 1980.
Pietrafesa, L. J., L. P. Atkinson, and J. O. Blanton, Evidence for deflection of the Gulf Stream by the Charleston rise, *Gulfstream; 4*(a), 3–7, 1978.
Rooney, D. M., G. S. Janowitz, and L. J. Pietrafesa, A simple model of deflection of the Gulf Stream by the Charleston rise, *Gulfstream, 4*(11), 3–7, 1978.
Schmitz, W. J., Jr., and P. P. Niiler, A note on the kinetic energy exchange between fluctuations and mean flow in the surface layer of the Florida Current, *Tellus, 11*, 814–819, 1969.
Schmitz, W. J., Jr., and W. S. Richardson, On the transport of the Florida Current, *Deep Sea Res., 15*, 675–693, 1968.
Stommel, H. M., *The Gulf Stream*, University of California Press, Berkeley, California, 1965.
Szabo, D., and G. L. Weatherly, Energetics of the Kuroshio south of Japan. *J. Mar. Res., 37*, 531–556, 1979.
von Arx, W. S., Measurements of the oceanic circulation in temperature and tropical latitudes, *Natl. Res. Counc. U. S. Publ. 309*, 13–35, 1954.
von Arx, W. S., D. F. Bumpus, and W. S. Richardson, On the fine structure of the Gulf Stream front, *Deep Sea Res.*, 46–65, 1955.
Vukovich, F. M., and B. W. Crissman, Further studies of a cold eddy on the eastern side of the Gulf Stream using satellite data and ship data, *J. Phys. Oceanogr., 8*, 838–843, 1978.
Webster, F., A description of Gulf Stream meanders off Onslow Bay, *Deep Sea Res., 9*, 130–143, 1961*a*.
Webster, F., The effect of meanders on the kinetic energy balance of the Gulf Stream, *Tellus, 13*, 392–401, 1961*b*.
Webster, F., Measurement of eddy fluxes of momentum in the surface layer of the Gulf Stream. *Tellus, 17*, 239–245, 1965.

(Received May 20, 1982;
revised November 22, 1982;
accepted November 22, 1982.)